Molecular Phylogenetics and Evolution 161 (2021) 107165

Contents lists available at ScienceDirect

Molecular Phylogenetics and Evolution

journal homepage: www.elsevier.com/locate/ympev

Evolutionary impacts of introgressive hybridization in a rapidly evolving group of jumping spiders (F. Salticidae, *Habronattus americanus group*)

T.C. Bougie [a,b,*], A. Brelsford [b], M. Hedin [a]

[a] Dept. of Biology, San Diego State University, San Diego, CA 92182, United States
[b] Evolution, Ecology, and Organismal Biology Department, University of California Riverside, Riverside, CA 92521, United States

ARTICLE INFO

Keywords:
Habronattus
Introgressive hybridization
Speciation
Sexual selection
western United States

ABSTRACT

Introgressive hybridization can be a powerful force impacting patterns of evolution at multiple taxonomic levels. We aimed to understand how introgression has affected speciation and diversification within a species complex of jumping spiders. The *Habronattus americanus* subgroup is a recently radiating group of jumping spiders, with species now in contact after hypothesized periods of isolation during glaciation cycles of the Pleistocene. Effects of introgression on genomes and morphology were investigated using phylogenomic and clustering methods using RADseq, ultraconserved elements (UCEs), and morphological data. We characterized 14 unique species/morphs using non-metric multidimensional scaling of morphological data, a majority of which were not recovered as monophyletic in our phylogenomic analyses. Morphological clusters and genetic lineages are highly incongruent, such that geographic region was a greater predictor of phylogenetic relatedness and genomic similarity than species or morph identity. STRUCTURE analyses support this pattern, revealing clusters corresponding to larger geographic regions. A history of rapid radiation in combination with frequent introgression seems to have mostly homogenized the genomes of species in this system, while selective forces maintain distinct male morphologies. GEMMA analyses support this idea by identifying SNPs correlated with distinct male morphologies. Overall, we have uncovered a system at odds with a typical bifurcating evolutionary model, instead supporting one where closely related species evolve together connected through multiple introgression events, creating a reticulate evolutionary history.

1. Introduction

Introgressive hybridization (IH, or introgression), a process by which genetic material is exchanged across species boundaries (Gompert et al. 2008), can be a powerful evolutionary force at several taxonomic levels (Abbott et al. 2016). For example, IH may lead to divergent lineages sharing morphological features (Nadeau et al. 2013; Martin et al. 2013; Poelstra et al. 2014; Martin et al. 2019). While the cross-species transfer of phenotypic traits has been documented to result in prezygotic or postzygotic reproductive isolation (i.e. Jiggins et al. 2001, 2008), some lineages may not develop barriers to gene flow and will continue to hybridize. Ongoing hybridization has the potential to degrade classical species boundaries by enabling the exchange of genetic material across most areas of the genome, effectively homogenizing genomes of divergent lineages. In these cases, only small fractions of the genome are divergent, often coding for differences in phenotypes and species identity (Toews et al. 2016; Stryjewski and Sorenson 2017; Campagna et al. 2017; Brelsford et al. 2017; Martin et al. 2019). Complete disintegration of species boundaries is also possible, where there are no divergent areas between genomes leading to species collapse (e.g. Grant and Grant 2002; Taylor et al., 2005; Kleindorfer et al., 2014).

Because closely related species experiencing rapid diversification are highly prone to IH (Seehausen 2004; Abbott et al. 2013), it is not surprising that many studies identifying homogenized genomes have worked with systems experiencing a rapid radiation (Campagna et al. 2017; Stryjewski and Sorenson 2017; Toews et al. 2016; Brelsford et al. 2017). Recent research has suggested hybridization can generate substantial variation through recombination, which has been documented to play an important role in the generation of new phenotypes involved in sexual selection and species identity (Malinsky et al. 2015; Stryjewski and Sorenson 2017; Meier et al. 2017). Such phenotypic diversification may fuel rapid radiations, which can lead to more introgression and subsequently more novel phenotypes, resulting in a positive feedback loop increasing the propensity for introgression (e.g. Stryjewski and

* Corresponding author at: SDSU Department of Biology, Life Sciences North Room. 206, 5500 Campanile Dr. San Diego, CA 92182-4614, USA.
E-mail address: tbougie@sdsu.edu (T.C. Bougie).

https://doi.org/10.1016/j.ympev.2021.107165
Received 30 September 2020; Received in revised form 11 March 2021; Accepted 25 March 2021
Available online 30 March 2021

Sorenson 2017; Meier et al. 2017).

IH can obviously complicate reconstruction of evolutionary history, especially in rapidly radiating species complexes. Contemporary and historical introgression has the potential to produce conflicting tree topologies and poor resolution on short branches (Alexander et al. 2017). Shared genetic material resulting from IH will cause discordance between morphological and genetic datasets and between different genetic datasets (Cui et al. 2013; MacGuigan and Near, 2019). Historically, it has been difficult with limited genetic data to detect signals of discordance or distinguish between causes of discordant patterns (Maddison 1997; Degnan and Rosenberg 2009). However, genomic-scale data enables us to ask and answer questions surrounding the evolutionary impacts of introgression, even in historically challenging groups (Fontaine et al., 2015; Mallet et al. 2016).

A well-suited group to explore how introgression impacts species relationships in recent and rapidly diverging taxa is the jumping spider genus *Habronattus*, commonly known as paradise spiders. *Habronattus* is a species rich taxon (>100 described species) that diverged relatively recently – possibly less than 5 million years ago (Bodner and Maddison 2012). *Habronattus* have keen vision (Zurek et al. 2015) and adult males are famous for elaborate colored ornaments and courtship behavior (Masta and Maddison 2002; Elias 2003; Elias et al. 2006). Many of these important courtship characters are affected by hybridization, suggesting that IH likely affects patterns of mate selection. Affected characters are also useful in identifying hybrids (Griswold 1987; Maddison and Hedin 2003). In addition to morphological evidence of hybridization, several groups within *Habronattus* also show genetic/genomic evidence of hybridization (Masta 2000; Maddison and Hedin 2003; Hedin and Lowder 2009; Blackburn and Maddison 2014; Leduc-Robert and Maddison 2018; Hedin et al. 2020). *Habronattus* appears to have generally weak pre-mating isolation, which may allow and/or promote hybridization. Males court willingly with heterospecifics, and females sometimes show xenophilic mating preferences (Hebets and Maddison 2005; Elias et al. 2006; Blackburn and Maddison 2014;Taylor et al. 2017).

The *H. americanus* species group is a monophyletic group within *Habronattus* (Griswold 1987; Leduc-Robert and Maddison 2018). It is comprised of 10 described species found primarily in western North America (Griswold 1987), including a clade of five closely related species, herein called the "*americanus* subgroup" – *H. americanus, H. bulbipes, H. kubai, H. waughi,* and *H. sansoni*. The time to the most recent common ancestor (tMRCA) between *H. americanus* and *H. sansoni* was estimated to be around 200,000 years ago using secondary calibration (see Fig. 4, Hedin et al. 2020). However, documented cases of introgression between *americanus* subgroup members and members of its sister clade, the *tarsalis* subgroup may pull estimated divergence times closer to the present (Leduc-Robert and Maddison 2018). The *americanus* subgroup is mostly distributed across mountainous regions of western North America, but can be found at lower elevations at higher latitudes (e.g. beaches on the coast of OR, WA, and British Columbia). Distributions of the group have almost certainly been impacted by Pleistocene glaciation. Described species within the *americanus* subgroup show extensive geographic variation, where geographically separated populations differ in patterns of male ornamentation (Griswold 1987; Blackburn and Maddison 2014; see Fig. 1). In addition to geographic variants within species, there are several known interspecific hybrid zones in the Sierra Nevada and Cascade Mountains. Previous genetic studies have documented hybridization and introgression within the *americanus* subgroup, both between phenotypically divergent

Fig. 1. Digital images of *americanus* subgroup morphs (*except for the *amer* PC morph). *amer* P = *H. americanus* P form, *amer* PL = *H. americanus* PL form, *amer* PLE = *H. americanus* PLE form, *amer* PLC = *H. americanus* PLC form, *amer* PC = *H. americanus* PC form, Gunnison = newly described morph collected near Gunnison, CO, *kub* south = *H. kubai* southern form, *kub* north = *H. kubai* northern form, *bulb* = *H. bulbipes*, BSK = newly described brown form of *H. sansoni*/ *H. kubai* morph, Pahvant = newly described morph collected near Pahvant range, UT, *sans* white = *H. sansoni* white morph, *sans* red = *H. sansoni* red morph, SCC = *H. sansoni* Cedar City morph collected near Cedar City, UT. *sans* red photograph credit to Thomas Barbin, *amer* PLE, Gunnison, *kub* south, *kub* north, *bulb*, BSK, and *sans* white to Brendan Boyer, all other photos by M Hedin. Images not to scale. (For interpretation of the references to color in this figure legend, the reader is referred to the web version of this article.)

populations of the same species (Blackburn and Maddison 2014) and between two or more different species (Leduc-Robert and Maddison 2018).

Using genomic and morphological datasets, we aim to (1) characterize the extreme morphological diversity within *americanus* subgroup in the context of introgression, (2) explore the effects of introgression on genomic relationships of the *americanus* subgroup, (3) explore the role IH may play in the disintegration of species boundaries, and (4) discuss alternative models of divergence that could produce patterns recovered in our results. Our disintegration model refers to the breakdown of genetic divergence between different species, such that heterospecifics may contain only few divergent areas in the genome. Under this model, we expect frequent hybridization and introgression events between divergently evolving lineages throughout their evolution. We also predict that populations- regardless of species identity- in close geographic proximity will be more genetically similar to each other than to geographically-distant populations. As such, currently described species may not form monophyletic groups or exclusive genetic clusters, rather geography may be a better predictor of phylogenetic relatedness and genomic similarity.

2. Methods

2.1. Specimen collection

Sample sites include locations throughout the montane western United States and southwestern Canada, including the Rocky Mountains, Sierra Nevada Mountains and Cascade Mountains (**Appendix A**). Griswold (1987) described species in the *americanus* subgroup using morphological characters primarily of the male face, palps, and leg I; we collected specimens that matched each of these described species, except for *H. waughi,* geographically-isolated in eastern Canada. Because *americanus* subgroup members are highly morphologically variable, some included populations do not match previously described species diagnoses and are given new informal names based on their morphologies.

2.2. Morphological data collection and analysis

Twenty-seven discrete morphological characters were scored for specimens that also have genomic data available (Table 1**, Appendix B**). Our morphology sample includes 80 males representing 4 described species and 14 morphological variants (3*H. americanus* morphs described in Blackburn and Maddison 2017 and nine newly defined morphs- see Results). Following Blackburn and Maddison's (2017) method for defining *H. americanus* morphs, we defined (*a priori*) variants primarily by palp color, chelicerae hair bundle color, leg I color and length of leg I ventral hairs. We used additional characters of some described species (*H. kubai* and *H. sansoni*) to further define morph types for these groups. Griswold (1987) scored 164 male characters, of which we chose those most feasible for accurate scoring and those variable within the *americanus* subgroup, with the addition of the expanded tarsus character not present in Griswold's revision. Characters were scored by examining individuals preserved in 100% ethanol under a dissecting microscope. To summarize morphological variation and visualize morphological clusters, we performed a non-metric multidimensional scaling (NMDS) analysis using the metaMDS function in the R package Vegan v2.5–6.

2.3. Samples, RAD data collection & analysis

The molecular sample includes all specimens used for the morphological analysis with the addition of 9 individuals – 95 specimens total. These samples comprise several described species and morphological variants recovered in our morphological analysis (see **Appendix A**). DNA extraction was performed using the Qiagen DNeasy Blood & Tissue

Table 1
Description of morphological characters and character states.

ID	Description	States
A	Crest above AER: long erect hairs above the AER form a row or crest along posterior margin of the AER. Erect "eyebrows."	0 = absent; 1 = present
B	Centrally located white setae above AME	States: 0 = absent; 1 = spot; 2 = stripe
C	Iridescent scales – pattern: variable within species, may have iridescent patches, or completely iridescent clypeus.	0 = absence of iridescent scales; 1 = full rectangular; 2 = flat center, flared at ends; 3 = 'm' shaped 4 = four broken segments; 5 = low, four connected segments; 6 = low single, long segment on bottom of clypeus
D	Clypeal covering emarginate: clypeus covered with two scale types and/or colors forming a well-marked white transverse band	0 = absent/no white band; 1 = spans entire length of AER; 2 = present only under AMEs; 3 = present only under ALEs; 4 = spans entire length of AER, but thicker towards the ALEs expanding down to the side of the iridescence
E	Color of non-iridescent setae on clypeus, NOT including white transverse band if present.	0 = all of clypeus covered in iridescence; 1 = brown; 2 = black; 3 = black and white; 4 = black and tan; 5 = black, white, and red
F	Clypeal covering divided in center	States: 0 = absent/not divided; 1 = divided
G	Clypeus with vertical bands that extends above AER: clypeal integument marked with dark vertical bands that may between AME and ALE to oral margin, with pale vertical band between these.	0 = no banding pattern; 1 = two dark bands above AMEs (SCC) only; 2 = two dark bands extending from above AMEs to oral margin; 3 = two dark bands extending from above AMEs to just below AMEs, 4 = two dark vertical bands extending from above AMEs to oral margin bisected with red bands
H	Color of hair pencils/hairs covering chelicerae	States: 0 = blue; 1 = red; 2 = pale/white; 3 = yellow/gold; 4 = no hair pencils; 5 = dull red
I	Presence of hair pencils covering chelicerae	States: 0 = absent; 1 = present; 2 = present, but very thin; 3 = present, but halfway cover the chelicerae
J	Leg I femur: Ventral fringe of elongate scales	States: 0 = absent; 1 = present
K	Leg I femur: Color of ventral side	0 = brown/dark; 1 = white/pale; 2 = yellow; 3 = orange + white; 4 = red; 5 = speckled tan and black; 6 = rusty red
L	Leg I femur: pattern	States: 0 = longitudinally striped; 1 = speckled; 2 = plain; 3 = cross between speckled and striped
M	Leg I tibia: Ventral fringe of elongate scales	States: 0 = absent; 1 = present
N	Leg I tibia: Color of ventral side	States: 0 = brown/dark; 1 = white/pale; 2 = yellow; 3 = orange; 4 = red, 5 = speckled tan and black; 6 = rusty red
O	Leg I tibia: pattern	States: 0 = longitudinally striped; 1 = speckled; 2 = plain, 3 = cross between speckled and striped
P	Leg I tarsus: expanded tarsus	States: 0 = absent; 1 = present
Q	Leg II femur: Ventral fringe of elongate scales	States: 0 = absent; 1 = present
R	Leg II femur: Color of ventral side	States: 0 = brown; 1 = white/pale; 2 = yellow; 3 = orange; 4 = red, 5 = speckled tan and black; 6 = rusty red
S	Leg II femur: pattern	States: 0 = longitudinally striped; 1 = speckled; 2 = plain; 3 = cross between speckled and striped
T	Leg III and IV pattern	States: 0 = longitudinally striped; 1 = speckled; 2 = plain

(*continued on next page*)

Table 1 (*continued*)

ID	Description	States
U	Palpal patella color	States: 0 = uniform, yellow/gold; 1 = uniform, white/pale; 2 = uniform, red; 3 = nonuniform, red/white; 4 = nonuniform, speckled tan and black; 5 = nonuniform, mostly black/some red/minimal white; 6 = nonuniform, black and pale/white; 7 = nonuniform brown and white; 8 = nonuniform brown and yellow; 9 = dip dyed red
V	Color of hairs covering tarsal bulb	0 = uniform, yellow/gold; 1 = uniform, white/pale; 2 = uniform, red; 3 = nonuniform, red with distinct white stripe; 4 = nonuniform, speckled tan and black, 5 = nonuniform, white/pale and orange
W	Presence of long, extended hairs covering tarsal bulb	0 = absent; 1 = present

protocol (Qiagen, Valencia, CA). Two to three legs were used for extraction, unless legs were unavailable, then the dorsal half of the cephalothorax was used. All genomic DNA extractions were quantified using a Qubit Fluorometer and quality of extractions was assessed using gel electrophoresis. We used both target capture of ultraconserved elements (UCEs) and double digest restriction-site associated DNA sequencing (ddRADseq) to gather genomic-scale data.

The ddRADseq dataset includes 95 specimens (see **Appendix A**). We followed a modified version of the Peterson et al. (2012) protocol, using SbfI and MseI enzymes. This enzyme combination was chosen to increase sequencing depth while accounting for the large genome sizes of *Habronattus* (~5.7 pg; Gregory, 2003). Sequencing was completed using 150PE reads on an Illumina Hiseq4000 platform at the University of California Berkeley's QB3 Vincent J. Coates Genomics Sequencing Laboratory.

Raw ddRADseq data were demultiplexed using STACKS v2.3.0 with default settings. The remaining data assembly was completed using iPYRAD v.0.7.30 (Eaton and Overcast 2020). All iPYRAD settings were left as default, with the exception of the clustering threshold for de novo assembly, set to 90% and the maximum number of indels allowed in a locus, which was set to 5. We created several alignments requiring data for different numbers of individuals in order to retain that locus in the alignment. These include alignments requiring loci to be shared by at least 48 (minsamp48), 24 (minsamp24), 10 (minsamp10), and 4 (minsamp4) individuals (similar to MacGuigan and Near, 2019). We also created two smaller alignments that contained fewer samples. The "trimmed" alignment included 67 samples, with a subsampling of individuals from three heavily collected sites (Sonora Pass, Mt. Ashland, and Mt. Hood), in attempt to reduce any sampling bias. The "core" alignment included the minimum number of individuals needed to account for morphological and geographic diversity (n = 40 samples) and required loci to be shared by at least half the samples (24).

We estimated phylogenomic relationships with ddRADseq data using concatenated and coalescent approaches. We concatenated each of the four complete alignments (minsamp 48, minsamp 24, minsamp 10, and minsamp 4) and the core alignment and completed maximum likelihood tree reconstructions for each minsamp dataset using IQ-TREE v1.2.1 (Nguyen et al. 2015). Branch support was estimated using the ultrafast bootstrap method (Hoang et al. 2018). We ran IQ-TREE with ModelFinder to estimate the correct substitution model (Kalyaanamoorthy et al. 2017). We performed constrained analyses in IQ-TREE v2.0.0 to identify whether our molecular data included any phylogenetic signal (similar to Willis et al. 2013) and to test different topology hypotheses. Two different constrained phylogenetic analyses were completed using each minsamp concatenated alignment and best fit substitution model estimated by ModelFinder. Constraint 1 required currently described species to form individual clades, without any constraints on internal nodes. Constraint 2 required currently described species to form individual clades, with the addition that morphological variants within each described species were also constrained as clades nested within the species clade. We performed the Shimodaira-Hasegawa (SH test; Shimodaira and Hasegawa 1999) and Kishino-Hasegawa (KH test; Kishino and Hasegawa 1989) tree topology tests implemented in IQ-TREE v2.0 to identify the topology with the highest likelihood score. Species trees for the minsamp datasets were also inferred using unlinked SNPs under the multi-species coalescent using *tetrad* implemented in IQTREE v1.2.1 (Nguyen et al. 2015). For each *tetrad* analysis, we sampled all quartets and ran 100 bootstrap replicates. Resulting trees were plotted using a custom R script.

We conducted two STRUCTURE 2.3.4 (Pritchard et al. 2000) analyses under non-admixture and admixture models using the trimmed data matrix of 67 individuals and 810 unlinked SNPs. STRUCTURE was run for clusters K = 2 to K = 10, each replicated 10 times. Each run included 100,000 generations with the first 10,000 removed as burnin. We used CLUMPAK (Kopelman et al. 2015) to summarize results. Optimal K values were chosen based on the prob(k) method (Pritchard et al. 2000), and we used a custom R script to plot pie charts of admixture proportions onto a map corresponding to sample locations.

To identify possible SNPs associated with each of the 14 morphs, we performed a GEMMA analysis (Zhou and Stephens 2012) on both the minsamp48 unlinked SNPs and all SNPs datasets. Within GEMMA, we used univariate linear mixed models (LMM) to perform the Wald association test, which can identify significant associations between SNPs and a predefined phenotype. We adjusted p-values for each dataset using the more conservative Bonferroni correction to correct for multiple comparisons; corrected p-values for the unlinked SNPs dataset was 0.0000768 and 0.00000421 for the all SNPs dataset. Results were graphed using a custom R script.

2.4. UCE data collection & analysis

The UCE dataset includes 16 ingroup samples from the four *americanus* group species used in morphological analysis and two outgroup individuals (*H. tuberculatus* and *H. aestus*; see **Appendix A**). UCE ingroup specimens were chosen to cover the geographic range of the subgroup, but do not include all morphological variants defined in the morphological analysis. We used the UCE probe set designed for Arachnida (Faircloth, 2016), with data collected and sequenced as in Hedin et al. (2020).

Raw UCE data were processed using the Phyluce pipeline (Faircloth, 2016). Assemblies were created using Trinity (Haas et al. 2013) within the Phyluce pipeline. Minimum coverage and maximum identity values for probe matching were set to 90. UCE loci were aligned with MAFFT and trimmed using Gblocks at settings: b1 = 0.5, b2 = 0.5, b3 = 8, b4 = 10. Alignments with less than 85% identical sites were flagged for manual examination and edited if necessary, using the program Geneious 11.0.4 (Biomatters). All loci were examined and corrected for large internal gaps in the conserved UCE region and obvious alignment errors.

IQ-TREE v2.0 was used to create a maximum likelihood concatenated UCE phylogeny with branch support estimated with the ultrafast bootstrap method (Nguyen et al. 2015; Hoang et al. 2018). We used ModelFinder implemented in IQ-TREE to estimate the best substitution model (Kalyaanamoorthy et al. 2017), presuming a single data partition. We measured genealogical concordance using the Concordance Factor function in IQ-Tree v2.0 (Minh et al. 2020). To estimate concordance factors, we used IQTREE to infer a maximum likelihood concatenated reference tree with 1000 bootstrap replicates on which concordance factors were annotated. In addition to calculating the gene concordance factor (gCF), this method can also calculate the site concordance factor (sCF), which is useful when gene alignments are relatively uninformative, creating uncertain gene trees (Minh et al. 2020). We suspect our individual UCE locus alignments may be relatively uninformative due to the recent divergence time and extensive gene flow between populations

in the *americanus* subgroup.

To test alternative topology hypotheses, we completed constrained analyses for the concatenated UCE dataset using IQ-TREE v2.0.0 using the best fit nuclear substitution model estimated by ModelFinder. We completed two constraint analyses as for the ddRAD data above and performed the KH and SH tree topology tests to identify the most likely topology of each minsamp dataset.

3. Results

3.1. Morphological analyses

Character scorings for all specimens are provided in **Appendix B**. The NMDS plot supports several distinct clusters corresponding loosely to assigned species identity or morph type (Fig. 2). There are two distinct *H. kubai* clusters, a south cluster – comprised of individuals collected in the central Sierra Nevada (*kub* south) and a north cluster – comprised of samples collected mostly from northern California and Southern Oregon (*kub* north), with the exception of two individuals collected from the central Sierra Nevada (HA0939 and HA1469). The *H. americanus* cluster occupies a large area of the NMDS plot, indicating substantial morphological diversity within this species. Previously defined morphs of *H. americanus* (P, PL, PLC, PC; Blackburn and Maddison 2014) fail to cluster together when all characters are analyzed, emphasizing high character variability in *H. americanus*. Based on our NMDS results in conjunction with previously defined morphological types, we identify 14 morphological forms: *kub* south, *kub* north, *sans* white, *sans* red, BSK, SCC, *bulb*, Pahvant, Gunnison, *amer* PLC, *amer* PL, *amer* P, *amer* PC, and *amer*PLE (**Appendix A**). The Pahvant, Gunnison, and BSK forms are newly identified morphs within the *americanus* subgroup and are not assigned a described species identity. A newly recognized *H. americanus* morph with an expanded tarsus on leg I was also discovered (*amer* PLE).

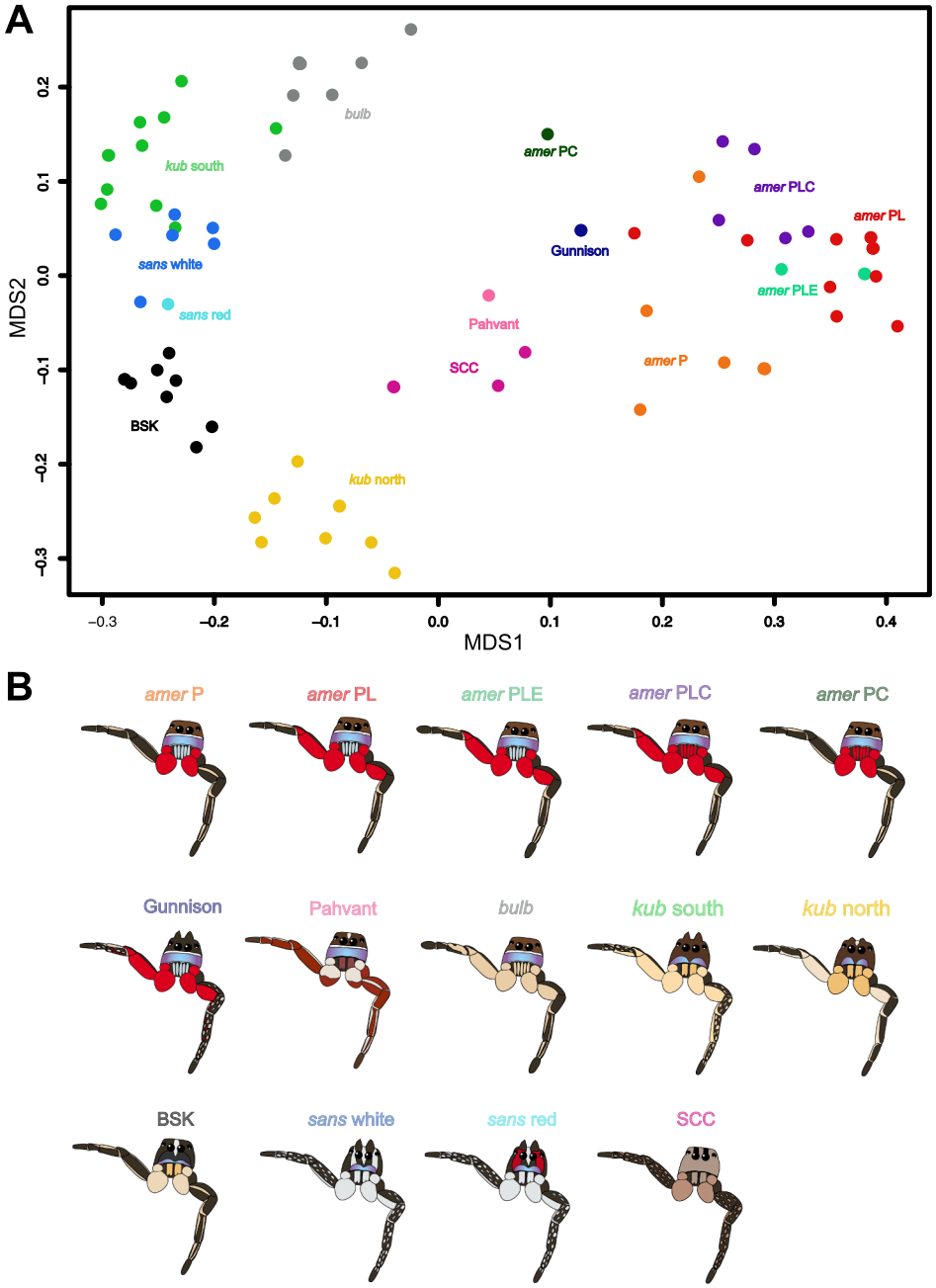

Fig. 2. Results of NMDS analysis of morphological data matrix (A) and cartoons of 14 species/morph identities (B).

3.2. ddRAD data & analysis

ddRADseq data was recovered for 95 out of 96 samples sequenced. Raw reads are available at the Short Read Archive (BioProject ID: PRJNA716323) and data matrices are available at Dryad (https://doi.org/10.6086/D16D6B). Our core dataset (minsamp = 20) included 1387 retained loci with an average of 983 loci per sample (**Appendix A**). Our trimmed dataset (minsamp = 33) included 814 retained loci with an average of 608 loci per sample. The complete sample datasets included 37687, 8406, 2374, and 655 retained loci after filtering for the minsamp4, minsamp10, minsamp24, and minsamp48 datasets, respectively.

ModelFinder estimated the best fit substitution model for the minsamp4 and minsamp10 datasets as TVM + F + R2 and TPM + F + R3 for the minsamp24 and minsamp48 datasets. IQTREE recovered similar topologies for each concatenated maximum likelihood phylogeny of the complete sample datasets despite different levels of missing data (Fig. 3; Supplemental Figs. 1–3). All four phylogenies identify four major lineages that loosely correspond with geography. The minsamp4, minsamp10, and minsamp24 phylogenies identify similar lineages: Rockies (RO), southern Oregon + northern California (SONC), and Sierra Nevada + southern California (SNSC), and a northern lineage composed of individuals from Oregon + Canada (NO). Lacking an outgroup, the minsamp4, 10, and 24 concatenated phylogenies were rooted between the NO and RO lineages. We chose to root at this branch because it establishes the monophyly of the NO lineage, placing northern *H. sansoni* individuals into a single clade. The minsamp48 phylogeny instead only fully supports the SNSC and NO lineages. The remaining two lineages (RO, SONC) are still present but became paraphyletic (Supplemental Fig. 3). Three specimens move between clades depending on the dataset (HA1123, HA1649, and HA1652). Support for deeper nodes increases with a lower minsamp value, likely due to number of sites used to construct the tree (more sites supporting a specific split = higher bootstrap support). The addition of more sequence data from RADseq methods has been documented to increase bootstrap support in a system that underwent a rapid radiation event (Wagner et al. 2013); the same could be occurring with our ddRADseq data. We refer to the four geographic groupings present in the minsamp4, 10, and 24 phylogenies moving forward.

The KH and SH topology tests supported topologies for the unconstrained minsamp phylogenies over both constraint topologies for each minsamp dataset (Table 2; constraint phylogenies for each minsamp dataset can be found in Supplemental Fig. 4–11).

Tetrad trees for each minsamp dataset yielded similar topologies to the concatenated IQTREE phylogenies (Supplemental Figures 12–15). Tetrad phylogenies were rooted similarly to concatenated phylogenies. All minsamp species trees recover four geographical lineages similar to the four geographic groupings (NO, RO, SONC, and SNSC) identified by the concatenated phylogenies. The same individuals that moved between clades in the IQTREE phylogenies (HA1123, HA1649, and HA1652) behave similarly in our Tetrad analyses, sometimes forming small clades of their own.

The optimal K value for the admixture STRUCTURE run was chosen

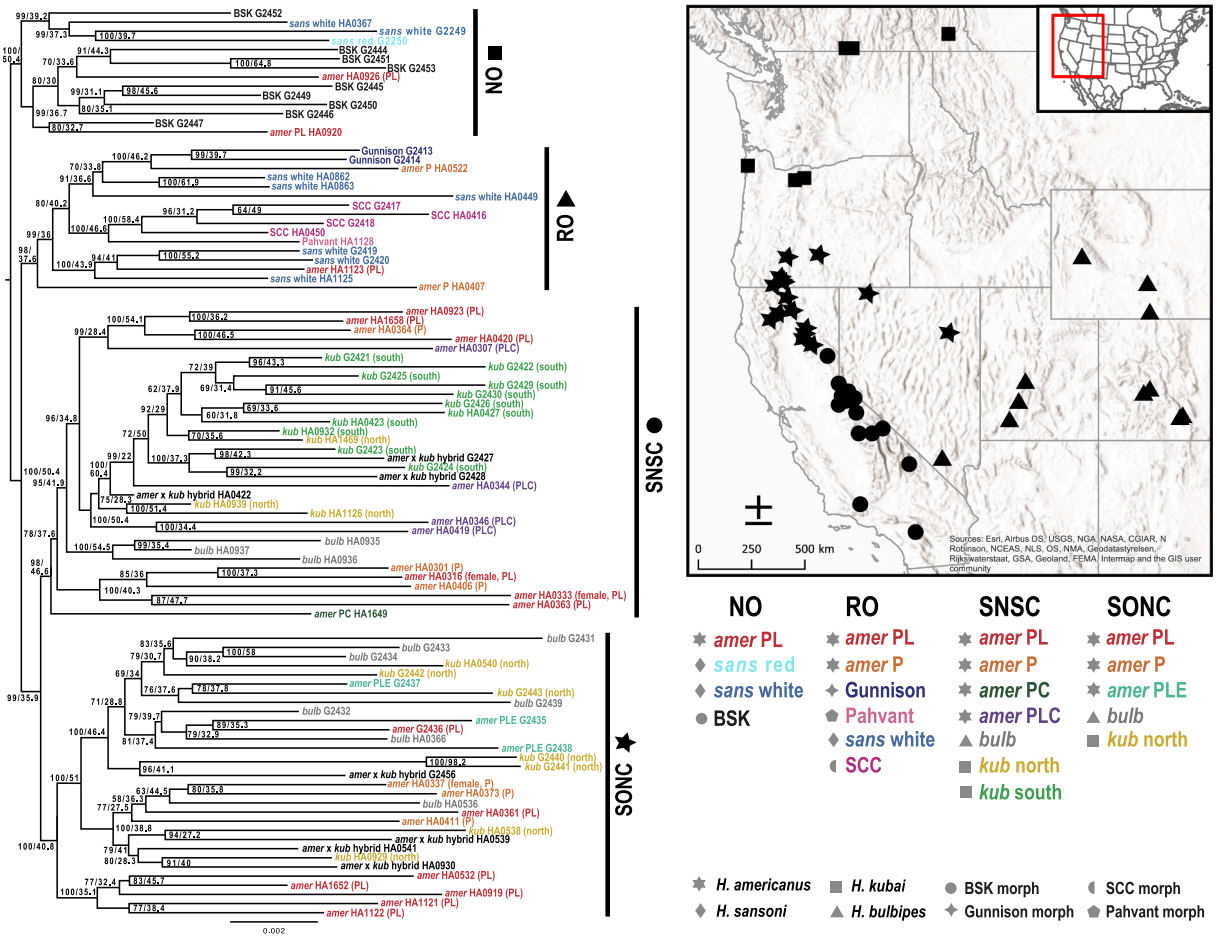

Fig. 3. Concatenated, unconstrained rooted ddRADseq minsamp 4 phylogeny with map denoting collection location of specimens in each lineage. Symbols on map correspond to symbols on lineage labels. Lower right denotes all forms present in each lineage, along with symbols in gray to denote described species each morph belongs to. Node labels show bootstrap support / sCF (in percentage of sites supporting split). Tip labels colored by morph/ species identity as in Fig. 2. SNSC = Sierra Nevada + Southern California clade, SONC = southern Oregon + northern California clade, RO = Rocky Mountain clade, NO = northern clade.

Table 2
Results of constrained tree analyses for all datasets. deltaL = log likelihood difference from the maximal log likelihood in the set. bp-Rell = bootstrap proportion using RELL method (Kishino et al.1990). p-KH = p-value of one sided Kishino-Hasegawa test (1989). p-SH = p-value of Shimodaira-Hasegawa test (2000). p-WKH = p-value of weighted KH test. p-WSH = p-value of weighted SH test. c-ELW = Expected Likelihood Weight (Strimmer and Rambaut, 2001). Plus signs denote the 95% confidence sets. Minus signs denote significant exclusion.

Dataset / Trees	Log Likelihood	deltaL	bp-RELL	p-KH	p-SH	p-WKH	p-WSH	c-ELW
UCE Trees								
Unconstrained	−151937.5826	0	1 +	1 +	1+	1+	1+	1 +
Constraint 1	−152197.5883	260.01	0 -	0 -	0 -	0 -	0 -	$1.96 * 10^{-52}$ -
Constraint 2	−152317.9014	380.32	0 -	0 -	0 -	0 -	0 -	$3.31 * 10^{-86}$ -
ddRAD Minsamp 4								
Unconstrained	−11190202.17	0	1 +	1+	1+	1+	1+	1+
Constraint 1	−11200698.81	10,497	0 -	0 -	0 -	0 -	0 -	0 -
Constraint 2	−11204447.28	14,245	0 -	0 -	0 -	0 -	0 -	0 -
ddRAD Minsamp 10								
Unconstrained	−2765208.566	0	1 +	1+	1+	1+	1+	1+
Constraint 1	−2773211.958	8003.4	0 -	0 -	0 -	0 -	0 -	0 -
Constraint 2	−2776162.114	10,954	0 -	0 -	0 -	0 -	0 -	0 -
ddRAD Minsamp 24								
Unconstrained	−884284.9398	0	1 +	1+	1+	1+	1+	1+
Constraint 1	−888737.6852	4452.7	0 -	0 -	0 -	0 -	0 -	0 -
Constraint 2	−890640.9283	6356	0 -	0 -	0 -	0 -	0 -	0 -
ddRAD Minsamp 48								
Unconstrained	−261217.5743	0	1 +	1+	1+	1+	1+	1+
Constraint 1	−263179.6385	1962.1	0 -	0 -	0 -	0 -	0 -	0 -
Constraint 2	−264235.2606	3017.7	0 -	0 -	0 -	0 -	0 -	0 -

as K = 3 (Fig. 4**c**). The three clusters align with geographic location and major phylogenetic lineages, with the exception of the disappearance of the NO lineage in which all NO individuals were included in the SONC cluster (purple). The optimal K value for the non-admixture STRUCTURE run was chosen as K = 4 (Supplemental Figure 16) The four genetic clusters generally follow geography and correspond with major lineages identified in the phylogenetic analyses. However, individuals collected in southern California are included in three different genetic clusters (NO, RO, SNSC).

GEMMA analyses identified between 0 and 10 significant SNPs in the unlinked SNPs dataset and between 0 and 159 significant SNPs in the all SNPs dataset. The *amer* PL morph had 0 significant SNPs in both datasets (Supplemental Figure 17 [all SNPs] and **18** [unlinked SNPs]). Without a reference genome, we cannot identify the genomic location of each significant SNP and are therefore unable to correlate these loci to any known candidate loci (e.g., color genes, etc.).

3.3. UCE data & analysis

We recovered 260 UCE loci with a mean length of 369 bp (**Appendix A)**. The mean number of parsimonious informative sites per locus was only 2.29, indicating that our UCE loci may be too conserved to successfully resolve phylogenetic relationships between populations and species. Raw reads are available at the Short Read Archive (BioProject ID: PRJNA719119) and data matrices are available at Dryad (https://doi.org/10.6086/D16D6B).

ModelFinder estimated the best-fit substitution model for the concatenated UCE alignment as TPM2u + F + R2. The concatenated UCE phylogeny is summarized in Fig. 4. Similar to ddRADseq phylogenetic analyses, the tree topology appears to reflect geography more than species or morph identity. Each of the four ingroup lineages – here referred to as SONC, Sierra Nevada, west Rockies, and 'A' lineage – includes at least two different species or morphs and most of the lineages contain individuals collected from specific geographic regions. The UCE lineages only loosely reflect those recovered in ddRADseq analyses. The largest difference being the absence of the NO clade, with individuals from that clade now included in the SONC clade (similar to STRUCTURE K = 3 results). Two individuals (HA0333 and HA0449) form the unlikely 'A' lineage, composed of samples collected in southern California and Colorado. The Sierra Nevada lineage includes samples from the central Sierra Nevada mountains, one sample from Wyoming and two British Columba samples; the latter three samples being discordant with the SNSC ddRAD lineage.

The gCF at many nodes appears to be low, ranging from 0% to 32.2% of loci supporting a node split, with all but two nodes below 10% of loci supporting a particular split. The sCF at each node ranges from 28.1% to 94% of sites supporting a particular split. KH and SH tree topology tests supported topologies for the unconstrained UCE phylogeny over both constraint topologies (Table 2**;** constraint UCE phylogenies can be found in Supplemental Figures 19 [const 1] and 20 [const2]).

4. Discussion

4.1. Morphological-genomic discordance

There is considerable morphological variation, both within and between *americanus* subgroup species. While species/morph specific clusters can be identified in our NMDS analysis, most clusters occupy large areas within the plot, highlighting within-morph diversity (Figs. 1 & 2). *Habronattus kubai* (*kub* south and *kub* north) and *H. sansoni* (*sans* white, *sans* red, and SCC) both form two distinctly separated clusters, implying morphological diversity within a described species. The NMDS also implies considerable morphological variation within *H. americanus,* however, it is more difficult to identify highly distinct morphological clusters than within *H. kubai* and *H. sansoni*. Although our morphological character matrix is smaller than that originally used by Griswold (1984), this matrix includes all variable characters within the *americanus* subgroup that could be reliably scored, with the exception of genitalia. Griswold (1984) found that genitalic diversity in the *americanus* subgroup is highly conserved; we doubt that inclusion of such data would identify more clearly separated clusters defined by described species.

Phylogenetic and clustering analysis of genomic data fails to mirror patterns reflected by morphology in *americanus* subgroup individuals. For example, on the ddRAD phylogeny the *kub* north morph is spread between both the SONC and SNSC lineages and the *amer* PL morph is included in all 4 genomic lineages (Fig. 3). Multiple *H. amer* PL morphs are spread throughout the UCE phylogeny and are intermixed with *sans* white and *kub* north morphs in some clades (Fig. 4). STRUCTURE analyses identify genetic clusters that include between three (SNSC) to five (RO and SONC) different species/morphs. All genomic clusters form somewhat geographically cohesive groups despite the number of

distinct morphs included within each cluster (Fig. 4**c**). Most morphological types are not monophyletic in the ddRAD and UCE phylogenies and several morphological types appear in multiple places across the phylogeny (Figs. 2-4). Constraint topologies that restrict clades to morphologically described species/morphs were never recovered as the most likely topology for any dataset (Table 2), supporting both signal in the genomic data, and discordance between morphology and genomic data.

4.2. Prior studies supporting introgression

A genus-wide transcriptome study identified evidence of introgression affecting phylogenetic relationships at several levels within *Habronattus*, including within and between species groups (Leduc-Robert and Maddison 2018). In particular, evidence supported admixture between members of the *americanus* group (see Fig. 4, Leduc-Robert and Maddison 2018). Evidence for intraspecific introgression within *H. americanus* in the Sierra Nevada has also been documented, where different *H. americanus* morphs remained divergent despite genome wide IH (Blackburn and Maddison 2014). Since previous studies did not include all *americanus* subgroup species and/or divergent morph types, effects of IH on specific phylogenetic relationships between members of the *americanus* subgroup were not examined.

Here, we identified patterns of geographically defined phylogenetic lineages within the *americanus* subgroup across different tree reconstruction methods, including the multispecies coalescent (MSC; Supplemental Figures 12–15). Traditionally, MSC approaches can be used to identify underlying patterns of divergence that might go undetected in concatenated datasets, because of the increased variance with the addition of many loci, or failure of concatenated approaches to identify signal from less variable loci (Maddison 1997; Willis et al. 2013). However, our tetrad species trees mostly coincided with concatenation results, supporting geographically defined genetic lineages.

UCE lineages also remain primarily defined by geographic location (Fig. 4). Small shifts in lineage composition from ddRADseq data is expected because of differences in number of samples, individuals included (species/morph and population identity), and lower resolution of the UCE data. The utility of UCEs to estimate phylogenetic relationships has been documented at multiple taxonomic levels, including recently diverged taxa (Smith et al. 2014; Starrett et al. 2017). However, our UCE data, like our ddRAD data, remained unable to detect the complete *americanus* subgroup speciation signal. Our phylogenomic analyses of both ddRADseq data and UCE data suggest that a homogenizing force is acting on the genomes of *americanus* subgroup members. Below we discuss alternative scenarios that may have led to genomic homogenization.

4.3. Competing models of divergence

We define our null hypothesis as one in close agreement with the taxonomy proposed by Griswold (1987) with four named species – *H. americanus* (all forms), *H. sansoni* (red and white forms), *H. kubai* (north and south forms), *H. bulbipes* – and four unnamed species – BSK, SCC, Gunnison, and Pahvant. We discuss below two alternative hypotheses that could explain the evolutionary patterns we recovered in the *americanus* subgroup (*although more might apply*): (A) species as defined above (i.e., the null hypothesis), with introgression within geographic centers, and (B) the *americanus* subgroup is instead comprised of four geographically localized, highly polymorphic species.

Null Hypothesis. Introgression within geographic centers

Introgression within geographic centers could explain the patterns we recovered in genomic and morphological datasets under our null hypothesis. The *americanus* subgroup is estimated at only 200,000 years old (Hedin et al. 2020), subjecting evolving populations to climatic shifts during the Pleistocene epoch (2,580,000 – 11,700 years ago). Previous studies in other systems suggest that climatic events during the Pleistocene likely isolated populations to smaller refugia, affecting population genetic structure, genetic diversity and lineage divergence (e.g., Hewitt 1996; Shafer et al., 2010; Hewitt 2011). As glacial ice retreated, population ranges likely expanded, possibly enabling contact with other previously isolated populations (Davis 2001). It is possible to imagine this scenario for *americanus* subgroup species, as they inhabit regions throughout western North America (Griswold 1987) that were affected by glaciation events. Additionally, several current hybrid zones are found at elevations that were likely covered in glacial ice as recently as the last glacial maximum (LGM), including Sonora Pass (~2700 m), Mt. Shasta (~2350 m), Mt. Ashland (~2000 m), and Mt. Hood (~960 m).

Climatic changes may have enabled *americanus* subgroup populations to come into secondary contact with divergently evolving populations following range expansions (e.g., Maddison and McMahon 2000); current hybrid zones may be testament to this. A lack of complete reproductive isolation between diverging *americanus* subgroup species/morphs could have allowed for IH, enabling gene exchange across species boundaries. In conjunction with a recent and rapid divergence, hybridization between species/morphs in close geographic proximity could explain our genomic results where we recovered lineages and admixture proportions defined by geographic location rather than morphological identity (Figs. 3, 4). We used the MSC in effort to identify underlying patterns of divergence that concatenation may have failed to identify. However, our species trees also failed to recover groups defined by morphology (Supplemental Figures 12–15). Rapid radiation events, like those that occurred within *Habronattus* (Leduc-Robert and Maddison 2018) encourage the retention of ancestral variation, causing conflicts between the most probable gene tree and the species branching pattern; this discordance is further exacerbated when hybridization is present (Maddison 1997).

Because sexual selection is believed to be strong in *Habronattus* (Peckham and Peckham 1889; Peckham and Peckham 1890; Masta and Maddison 2002; Elias 2003; Hebets and Maddison 2005; Elias et al. 2006; Elias et al. 2012), it may be expected that genomic regions underlying male phenotypes are under strong selection relative to other areas of the genome (e.g. male *Lycaeides* characters, Nice and Shapiro 1999; Nice et al. 2005; Gompert et al. 2008). If this is the case in the *americanus* subgroup, then selection has maintained male morphologies despite widespread genome homogenization. Our GEMMA results appear to support this scenario by identifying at least one significant SNP associated with each morph, aside from *amer* PL (Supplemental Figures 17 and 18). Although we cannot identify where in the genome these SNPs are located or what specific trait they are correlated with, these results are consistent with small genomic regions differentiating morphs in some way. Of course, our ddRAD loci are likely not dense enough to capture all SNPs associated with the morphs. We might also expect sexual selection to reinforce membership in species/morph clades. Instead, our results suggest that while sexual selection may be preserving divergent male phenotypes, widespread introgression in remaining parts of the genome could be swamping any speciation signal, resulting in a pattern of little correlation between species boundaries and genetic markers (similar to *Lycaeides*, Nice and Shapiro 1999; Nice 2005; Gompert et al. 2008). To summarize, if we accept the null hypothesis, *americanus* subgroup individuals likely speciated along color lines (male morphologies) followed by introgression within geographic regions, leading to rejection of a typical bifurcating evolutionary model (Gompert et al. 2014).

Alternative Hypothesis. americanus *subgroup taxa are composed of four polymorphic species*

This hypothesis rejects the current taxonomy, instead favoring the presence of four highly polymorphic species; these four species include SONC, SNSC, RO, and NO, unless noted otherwise. This scenario intuitively fits with our phylogenomic data where species lineages correlate with geography. High levels of morphological diversity in these species and shared morphs across species could have occurred via maintained

ancestral polymorphism at color loci, in a manner similar to that described by Jamie and Meier (2020). These authors describe three non-exclusive processes that could lead to identical polymorphisms across species: inheritance via ancestral variation, mutation, and introgression. Guerrero and Hahn (2017) describe how ancestral polymorphisms may remain present in descending species via a speciation sieve-like process, where balancing selection in an ancestral species eventually leads to fixation of different allelic classes in diverging lineages (see Fig. 1, Guerrero and Hahn 2017). If balancing selection is no longer acting on these alleles in descendent species, the result is blocks of highly diverged and selectively neutral haplotypes between species that can persist through several speciation events, resulting in species pairs sharing sieved regions (Campagna et al. 2017; Han et al. 2017).

Under the sieve hypothesis, each geographically defined *americanus* subgroup species may share neutral, fixed polymorphic alleles (and additional linked genes) near ancestral loci that were once under strong selection, which may include color traits. However, the likelihood that identical polymorphisms across species could be the only cause for such variation within and among species in the group seems unlikely. Differences in male morphs are determined by more than one trait and almost certainly more than one genetic locus. While reports of selection maintaining polymorphisms at a single locus and recurring in multiple members of a species radiation are well documented (see Table 1, Jamie and Meier 2020), few cases demonstrate this occurrence in a multilocus setting (Llaurens et al 2017), although still theoretically possible (Turelli and Barton 2004). We view it as unlikely that the loci responsible for morph variation in *americanus* subgroup species were both maintained from ancestral polymorphism and sieved in populations of each species in such a way that leads to a clear, congruent morphological pattern. However, if we accept that color polymorphisms could account for at least some of the morphological variation, such polymorphisms would need to be maintained. If polymorphisms were a result of a speciation sieve, they may be selectively neutral and easily remain in each species. Alternatively, some form of negative frequency dependent selection that is not dependent on a population's ecology (e.g. NFDS on alternative mating types) – ecologies shared across geographic regions (here species) are similar in many cases– could be responsible for maintaining polymorphisms across species (Jamie and Meier 2020). However, we currently have no evidence that any morph type has a selective benefit over others, likely ruling out convergence as a means responsible for identical morph types occurring in different genetic lineages.

Introgression, the third process that Jamie and Meier (2020) describe for shared polymorphisms across species, is present throughout the history of *Habronattus* (Masta 2000; Maddison and Hedin 2003; Hedin and Lowder 2009; Blackburn and Maddison 2014; Leduc-Robert and Maddison 2018; Hedin et al. 2020). Such IH could have introduced additional variation in the ancestor of the *americanus* subgroup. It is also possible that throughout the recent divergence of the four geographic species, some populations came into contact with others, enabling hybridization and subsequent introgression. Similar to our null hypothesis, biogeographic conditions could have brought diverging species together as the climate shifted, resulting in introgression of male color morphs to each of the four geographically defined species. Therefore, the four species may exhibit identical male morphological traits across species and highly variable traits within species due to both retention of ancestral polymorphism and introgression.

Our genomic data could support a scenario similar to the alternative hypothesis, although our STRUCTURE results would support only three "species" (Fig. 4) instead of the four recovered in our phylogenomic analyses (Fig. 3). This hypothesis assumes only four species that have extreme morphological diversity through retention of polymorphisms and/or gene flow via introgression. While this is a possibility, it seems unlikely considering that in most populations, there is only a single male morph represented. If we had highly polymorphic and morphologically

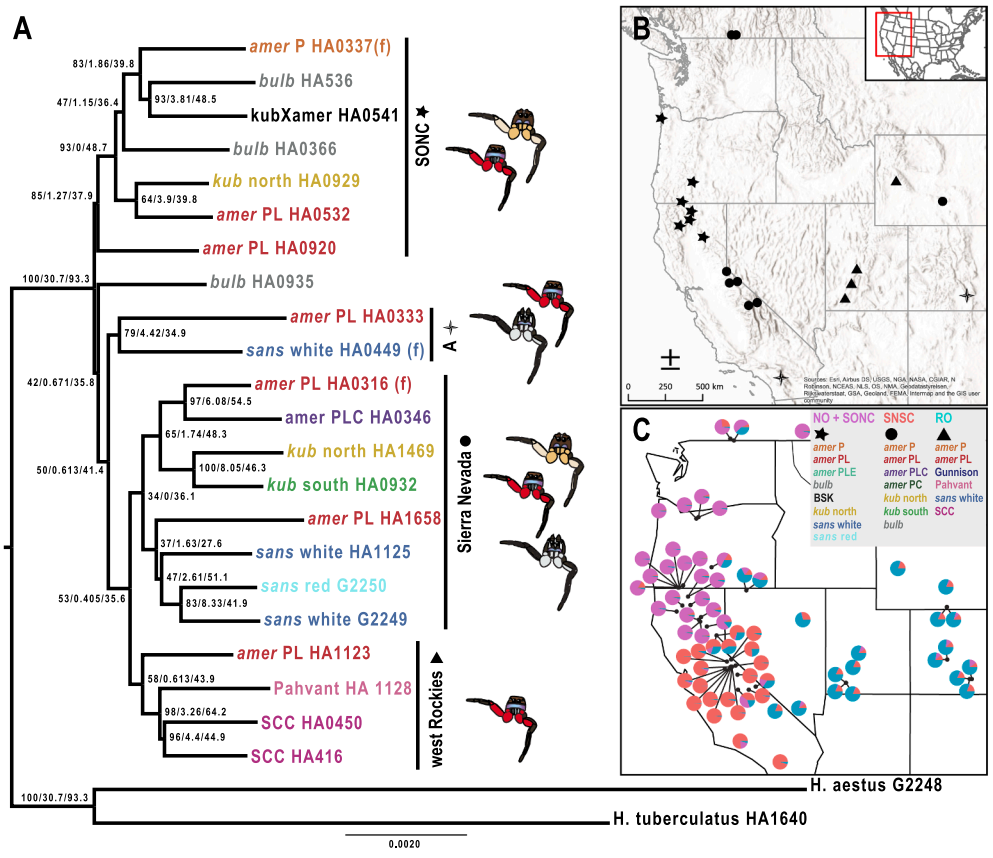

Fig. 4. (A) Concatenated, unconstrained rooted UCE phylogeny. Tip labels colored by morph/ species identity as in Fig. 2. Node labels show bootstrap support / gCF (in percentage of loci supporting split) / sCF (in percentage of sites supporting split). Cartoon *amer* PL, *kub* north, and *sans* white morphs shown to the right of all clades where each morph is present. (B) map denoting location where individuals in each lineage were collected, symbols on map reflect symbols on lineage labels. (C) Mapped admixture proportions estimated by STRUCTURE and shown as pie charts for the trimmed ddRADseq dataset. Upper right corner notes distinct species/morphs represented in each of the three clusters, ddRAD lineage names are color coordinated to denote which cluster they reflect most and UCE lineage symbols are listed beneath ddRAD lineage names to aid in comparison between the three analyses.

diverse species, with little evidence for any selective benefit of different male morphs, we might expect to see several morph types at a single collection locality. This occurrence is relatively rare, only observed at a few locations where different morph types hybridize.

5. Conclusions

Additional research is needed to identify whether the *americanus* subgroup speciated along color lines followed by introgression within geographic centers (null hypothesis) or along geographic lines with retention of polymorphism at a few color genes and/or introgression between diverging lineages (alternative hypothesis). Evidence presented here suggests that the former hypothesis is more likely, but we cannot confidently reject the latter. Identification of divergent genomic loci responsible for different male phenotypes could provide insight into speciation modes and how different morphs developed (Campagna et al. 2017). Mating experiments and additional population genetic analyses at hybrid zone sites could aid in identifying the directionality of gene flow – e.g. are *H. americanus* females promoting hybridization by choosing males of different species or are all *H. americanus* subgroup females choosing heterospecific mates? It is clear that many questions remain to be answered in this system. However, opportunities for future research could lead to new discoveries in speciation and evolutionary dynamics of rapidly radiating and highly diverse systems.

Regardless of the mode of divergence, it appears the *americanus* subgroup is evolving as a complex unit of closely related taxa. Currently described species and newly identified morphs might be categorized as "nascent" species – defined as recently-diverged lineages not yet having developed intrinsic reproductive isolation (Cutter and Gray 2016). Complete reproductive isolation has not yet been established in the *americanus* subgroup, as species readily hybridize in areas of sympatry, and the group appears to be very young. As such, *americanus* subgroup members share both characteristics of nascent species.

Frequent introgression between nascent species might make them susceptible to population fusion – an avenue leading to extinction (Rhymer and Simberloff 1996). It is possible that throughout the evolution of this group, some lineages succumbed to lineage fusion as gene flow from frequent introgression overwhelmed any divergent selection. Alternatively, frequent IH between evolving *americanus* subgroup members might have led to speciation through combinatorial mechanisms (Marques et al. 2019). As such, the same force that might have been creating nascent species also possibly reabsorbed nascent species in the *americanus* subgroup. This cycle of ephemeral speciation throughout the evolutionary history of this group could lead to the extreme genomic homogenization we identify today, where only small divergent areas of the genome responsible for species identity remain differentiated.

Systems experiencing rapid radiations and substantial hybridization challenge our current understanding of speciation and evolution. As introgression acts as a powerful force promoting radiation, it can be beneficial to think about each radiating cluster as a single community. The community is composed of closely related species that actively share genetic material and may compete for resources, but essentially evolve as a single lineage (Zhang et al., 2019). An increasing number of studies are calling into question the traditional bifurcating model of evolution/speciation, supporting instead a reticulate pattern with multifurcating branches (Abbott et al. 2013; Mallet et al. 2016; Wen et al. 2016). It appears as though the *americanus* subgroup falls into the category of a complex of closely related, nascent species evolving together through multiple introgression events creating a reticulate evolutionary history.

CRediT authorship contribution statement

T.C. Bougie: Conceptualization, Funding acquisition, Writing - original draft, Data curation, Investigation, Formal analysis, Visualization. **A. Brelsford:** Supervision, Funding acquisition, Resources. **M. Hedin:** Conceptualization, Supervision, Funding acquisition, Writing - review & editing, Data curation, Resources, Validation.

Declaration of Competing Interest

The authors declared that there is no conflict of interest.

Acknowledgements

Permits for specimen collection were granted by the California Department of Fish and Wildlife (SC-190110005). We thank E. Henderson, D. Pierce, and M. Sankovitz for assistance in RADseq data collection. Several individuals helped collect specimens, including P. Abbott, M. Baker, E. Ciaccio, D. Deeb Dre, C. Hayashi, C. Isip, D. Kavanaugh, R. Keith, D. Leavitt, M. Lowder, D. Maddison, J. Maddison, W. Maddison, S. Masta, K. Ober, H. Proctor, E. Selvidge, and J. Starrett. Funding was provided by grants to TB (American Arachnological Society, University of California, Riverside, Society for Systematic Biologists)and MH (NSF DEB 1754591).

Appendix A. Supplementary data

Supplementary data to this article can be found online at https://doi.org/10.1016/j.ympev.2021.107165.

References

Abbott, R., Albach, D., Ansell, S., Arntzen, J.W., Baird, S.J.E., Bierne, N., Boughman, J., Brelsford, A., Buerkle, C.A., Buggs, R., Butlin, R.K., Dieckmann, U., Eroukhmanoff, F., Grill, A., Cahan, S.H., Hermansen, J.S., Hewitt, G., Hudson, A.G., Jiggins, C., Jones, J., Keller, B., Marczewski, T., Mallet, J., Martinez-Rodriguez, P., Möst, M., Mullen, S., Nichols, R., Nolte, A.W., Parisod, C., Pfennig, K., Rice, A.M., Ritchie, M.G., Seifert, B., Smadja, C.M., Stelkens, R., Szymura, J.M., Väinölä, R., Wolf, J.B.W., Zinner, D., 2013. Hybridization and speciation. J. Evol. Biol. 26 (2), 229–246. https://doi.org/10.1111/j.1420-9101.2012.02599.x.

Abbott, R.J., Barton, N.H., Good, J.M., 2016. Genomics of hybridization and its evolutionary consequences. Mol. Ecol. 25 (11), 2325–2332. https://doi.org/10.1111/mec.13685.

Alexander, A.M., Su, Y.-C., Oliveros, C.H., Olson, K.V., Travers, S.L., Brown, R.M., 2017. Genomic data reveals potential for hybridization, introgression, and incomplete lineage sorting to confound phylogenetic relationships in an adaptive radiation of narrow-mouth frogs: Brief Communication. Evol. 71 (2), 475–488. https://doi.org/10.1111/evo.13133.

Blackburn, G.S., Maddison, W.P., 2014. Stark sexual display divergence among jumping spider populations in the face of gene flow. Mol. Ecol. 23 (21), 5208–5223. https://doi.org/10.1111/mec.12942.

Brelsford, A., Toews, D.P.L., Irwin, D.E., 2017. Admixture mapping in a hybrid zone reveals loci associated with avian feather coloration. P. Royal Soc. B: Biol. Sci. 284 (1866), 20171106. https://doi.org/10.1098/rspb.2017.1106.

Campagna, L., Repenning, M., Silveira, L.F., Fontana, C.S., Tubaro, P.L., Lovette, I.J., 2017. Repeated divergent selection on pigmentation genes in a rapid finch radiation. Sci. Adv. 3 (5), e1602404 https://doi.org/10.1126/sciadv.1602404.

Cui, R., Schumer, M., Kruesi, K., Walter, R., Andolfatto, P., Rosenthal, G.G., 2013. Phylogenomics reveals extensive reticulate evolution in *Xiphophorus* fishes: phylogenomics of *Xiphophorus* fishes. Evolution 67 (8), 2166–2179. https://doi.org/10.1111/evo.12099.

Cutter, A.D., Gray, J.C., 2016. Ephemeral ecological speciation and the latitudinal biodiversity gradient: perspective. Evolution 70 (10), 2171–2185. https://doi.org/10.1111/evo.13030.

Davis, M.B., 2001. Range Shifts and Adaptive Responses to Quaternary Climate Change. Science 292 (5517), 673–679. https://doi.org/10.1126/science.292.5517.673.

Degnan, J.H., Rosenberg, N.A., 2009. Gene tree discordance, phylogenetic inference and the multispecies coalescent. Trends. Evol. 24 (6), 332–340. https://doi.org/10.1016/j.tree.2009.01.009.

Eaton D.A.R, Overcast I., 2020. ipyrad: Interactive assembly and analysis of RADseq datasets. http://ipyrad.readthedocs.io.

Elias, D.O., 2003. Seismic signals in a courting male jumping spider (Araneae: Salticidae). J. Exp. Biol. 206 (22), 4029–4039. https://doi.org/10.1242/jeb.00634.

Elias, Damian O., Hebets, E.A., Hoy, R.R., 2006. Female preference for complex/novel signals in a spider. Behav. Ecol. 17 (5), 765–771. https://doi.org/10.1093/beheco/arl005.

Elias, D.O., Maddison, W.P., Peckmezian, C., Girard, M.B., Mason, A.C., 2012. Orchestrating the score: complex multimodal courtship in the *Habronattus coecatus* group of *Habronattus* jumping spiders (Araneae: Salticidae): multimodal courtship in *Habronattus*. Biol. J. Linn. Soc. 105 (3), 522–547. https://doi.org/10.1111/j.1095-8312.2011.01817.x.

Faircloth, B.C., 2016. PHYLUCE is a software package for the analysis of conserved genomic loci. Bioinformatics 32, 786–788.

Fontaine, M.C., Pease, J.B., Steele, A., Waterhouse, R.M., Neafsey, D.E., Sharakhov, I.V., Jiang, X., Hall, A.B., Catteruccia, F., Kakani, E., Mitchell, S.N., Wu, Y.-C., Smith, H. A., Love, R.R., Lawniczak, M.K., Slotman, M.A., Emrich, S.J., Hahn, M.H., Besansky, N.J., 2015. Extensive introgression in a malaria vector species complex revealed by phylogenomics. Science 347 (6217), 1258524. https://doi.org/10.1126/science.1258524.

Gompert, Z., Forister, M.L., Fordyce, J.A., Nice, C.C., 2008. Widespread mito-nuclear discordance with evidence for introgressive hybridization and selective sweeps in *Lycaeides*. Mol. Ecol. 17 (24), 5231–5244. https://doi.org/10.1111/j.1365-294X.2008.03988.x.

Gompert, Z., Lucas, L.K., Buerkle, C.A., Forister, M.L., Fordyce, J.A., Nice, C.C., 2014. Admixture and the organization of genetic diversity in a butterfly species complex revealed through common and rare genetic variants. Mol. Ecol. 23 (18), 4555–4573. https://doi.org/10.1111/mec.12811.

Grant, P.R., 2002. Unpredictable Evolution in a 30-Year Study of Darwin's Finches. Science 296 (5568), 707–711. https://doi.org/10.1126/science.1070315.

Gregory, T.R., 2003. Genome Sizes of Spiders. J. Hered. 94 (4), 285–290. https://doi.org/10.1093/jhered/esg070.

Griswold, C.E., 1987. A revision of the jumping spider genus Habronattus F.O.P. Cambridge (Araneae; Salticidae), with phenetic and cladistic analyses. Univ. California Pub. Ent. 107, 1–344.

Guerrero, R.F., Hahn, M.W., 2017. Speciation as a sieve for ancestral polymorphism. Mol. Ecol. 26 (20), 5362–5368. https://doi.org/10.1111/mec.14290.

Haas, B.J., Papanicolaou, A., Yassour, M., Grabherr, M., Blood, P.D., Bowden, J., Couger, M.B., Eccles, D., Li, B., Lieber, M., MacManes, M.D., Ott, M., Orvis, J., Pochet, N., Strozzi, F., Weeks, N., Westerman, R., William, Thomas, Dewey, C.N., Henschel, R., LeDuc, R.D., Friedman, N., Regev, A., 2013. De novo transcript sequence reconstruction from RNA-seq using the Trinity platform for reference generation and analysis. Nat. Protoc. 8 (8), 1494–1512. https://doi.org/10.1038/nprot.2013.084.

Han, F., Lamichhaney, S., Grant, B.R., Grant, P.R., Andersson, L., Webster, M.T., 2017. Gene flow, ancient polymorphism, and ecological adaptation shape the genomic landscape of divergence among Darwin's finches. Genome Res. 27 (6), 1004–1015. https://doi.org/10.1101/gr.212522.116.

Hebets, E.A., Maddison, W.P., 2005. Xenophilic mating preferences among populations of the jumping spider *Habronattus pugillis* Griswold. Behav. Ecol. 16 (6), 981–988. https://doi.org/10.1093/beheco/ari079.

Hedin, M., Foldi, S., Rajah-Boyer, B., 2020. Evolutionary divergences mirror Pleistocene paleodrainages in a rapidly-evolving complex of oasis-dwelling jumping spiders (Salticidae, *Habronattus tarsalis*). Mol. Phylogenet. Evol. 144, 106696 https://doi.org/10.1016/j.ympev.2019.106696.

Hedin, M., Lowder, M.C., 2009. Phylogeography of the *Habronattus* amicus species complex (Araneae: Salticidae) of western North America, with evidence for localized asymmetrical mitochondrial introgression. Zootaxa. 2307 (1), 39–60. https://doi.org/10.11646/zootaxa.2307.1.2.

Hewitt, G., 1996. Some genetic consequences of ice ages, and their role in divergence and speciation. Biol. J. Linn. Soc. 58 (3), 247–276. https://doi.org/10.1006/bijl.1996.0035.

Hewitt, G.M., 2011. Quaternary phylogeography: the roots of hybrid zones. Genetica 139 (5), 617–638. https://doi.org/10.1007/s10709-011-9547-3.

Hoang, D.T., Chernomor, O., von Haeseler, A., Minh, B.Q., Vinh, L.S., 2018. UFBoot2: Improving the ultrafast bootstrap approximation. Mol. Biol. Evol. 35 (2), 518–522. https://doi.org/10.1093/molbev/msx281.

Jamie, G.A., Meier, J.I., 2020. The Persistence of Polymorphisms across Species Radiations. Trends Ecol. Evol. S0169534720301117 https://doi.org/10.1016/j.tree.2020.04.007.

Jiggins, C.D., Naisbit, R.E., Coe, R.L., Mallet, J., 2001. Reproductive isolation caused by colour pattern mimicry. Nature 411 (6835), 302–305. https://doi.org/10.1038/35077075.

Jiggins, C.D., Salazar, C., Linares, M., Mavarez, J., 2008. Hybrid trait speciation and *Heliconius* butterflies. Philos. T. R. Soc. B: Biol. Sci. 363 (1506), 3047–3054. https://doi.org/10.1098/rstb.2008.0065.

Kishino, H., Hasegawa, M., 1989. Evaluation of the maximum likelihood estimate of the evolutionary tree topologies from DNA sequence data, and the branching order in *Hominoidea*. J. Mol. Evol. 29 (2), 170–179. https://doi.org/10.1007/BF02100115.

Kleindorfer, S., O'Connor, J.A., Dudaniec, R.Y., Myers, S.A., Robertson, J., Sulloway, F.J., 2014. Species collapse via hybridization in Darwin's tree finches. Am. Nat. 183 (3), 325–341. https://doi.org/10.1086/674899.

Kopelman, N.M., Mayzel, J., Jakobsson, M., Rosenberg, N.A., Mayrose, I., 2015. Clumpak : a program for identifying clustering modes and packaging population structure inferences across K. Mol. Ecol. Resour. 15 (5), 1179–1191. https://doi.org/10.1111/1755-0998.12387.

Leduc-Robert, G., Maddison, W.P., 2018. Phylogeny with introgression in *Habronattus* jumping spiders (Araneae: Salticidae). BMC Evol. Biol. 18 (1), 24. https://doi.org/10.1186/s12862-018-1137-x.

Llaurens, V., Whibley, A., Joron, M., 2017. Genetic architecture and balancing selection: the life and death of differentiated variants. Mol. Ecol. 26 (9), 2430–2448. https://doi.org/10.1111/mec.14051.

MacGuigan, D.J., Near, T.J., 2019. Phylogenomic signatures of ancient introgression in a rogue lineage of darters (Teleostei: Percidae). Syst. Biol. 68 (2), 329–346. https://doi.org/10.1093/sysbio/syy074.

Maddison, W., Hedin, M., 2003. Phylogeny of *Habronattus* jumping spiders (Araneae: Salticidae), with consideration of genital and courtship evolution: *Habronattus* spider phylogeny. Syst. Entomol. 28 (1), 1–22. https://doi.org/10.1046/j.1365-3113.2003.00195.x.

Maddison, W.P., 1997. Gene trees in species trees. Syst. Biol. 14 (3), 523–536.

Maddison, W., McMahon, M., 2000. Divergence and reticulation among montane populations of a jumping spider (*Habronattus pugillis* Griswold). System. Biol. 49 (3), 400–421.

Malinsky, M., Challis, R.J., Tyers, A.M., Schiffels, S., Terai, Y., Ngatunga, B.P., Miska, E. A., Durbin, R., Genner, M.J., Turner, G.F., 2015. Genomic islands of speciation separate cichlid ecomorphs in an East African crater lake. Science 350 (6267), 1493–1498. https://doi.org/10.1126/science.aac9927.

Mallet, J., Besansky, N., Hahn, M.W., 2016. How reticulated are species? BioEssays 38 (2), 140–149. https://doi.org/10.1002/bies.201500149.

Marques, D.A., Meier, J.I., Seehausen, O., 2019. A combinatorial view on speciation and adaptive radiation. Trends Ecol. Evol. 34 (6), 531–544. https://doi.org/10.1016/j.tree.2019.02.008.

Martin, S.H., Dasmahapatra, K.K., Nadeau, N.J., Salazar, C., Walters, J.R., Simpson, F., Blaxter, M., Manica, A., Mallet, J., Jiggins, C.D., 2013. Genome-wide evidence for speciation with gene flow in *Heliconius* butterflies. Genome Res. 23 (11), 1817–1828. https://doi.org/10.1101/gr.159426.113.

Martin, S.H., Davey, J.W., Salazar, C., Jiggins, C.D., 2019. Recombination rate variation shapes barriers to introgression across butterfly genomes. PLoS Biol. 17 (2), e2006288 https://doi.org/10.1371/journal.pbio.2006288.

Masta, S.E., Maddison, W.P., 2002. Sexual selection driving diversification in jumping spiders. Proc. Natl. Acad. Sci. 99 (7), 4442–4447. https://doi.org/10.1073/pnas.072493099.

Meier, J.I., Marques, D.A., Mwaiko, S., Wagner, C.E., Excoffier, L., Seehausen, O., 2017. Ancient hybridization fuels rapid cichlid fish adaptive radiations. Nat. Commun. 8 (1), 14363. https://doi.org/10.1038/ncomms14363.

Minh, B.Q., Hahn M.W., Lanfear, R., 2020. New methods to calculate concordance factors for phylogenomic datasets. Mol. Biol. Evol. in press. https://doi.org/10.1093/molbev/msaa106.

Nadeau, N.J., Martin, S.H., Kozak, K.M., Salazar, C., Dasmahapatra, K.K., Davey, J.W., Baxter, S.W., Blaxter, M.L., Mallet, J., Jiggins, C.D., 2013. Genome-wide patterns of divergence and gene flow across a butterfly radiation. Mol. Ecol. 22 (3), 814–826. https://doi.org/10.1111/j.1365-294X.2012.05730.x.

Nguyen, L.-T., Schmidt, H.A., von Haeseler, A., Minh, B.Q., 2015. IQ-TREE: A fast and effective stochastic algorithm for estimating maximum-likelihood phylogenies. Mol. Biol. Evol. 32 (1), 268–274. https://doi.org/10.1093/molbev/msu300.

Nice, C.C., Shapiro, A.M., 1999. Molecular and morphological divergence in the butterfly genus *Lycaeides* (Lepidoptera: Lycaenidae) in North America: evidence of recent speciation. J. Evol. Biol. 12 (5), 936–950. https://doi.org/10.1046/j.1420-9101.1999.00111.x.

Nice, C.C., Anthony, N., Gelembiuk, G., Raterman, D., Ffrench-Constant, R., 2005. The history and geography of diversification within the butterfly genus *Lycaeides* in North America. Mol. Ecol. 14 (6), 1741–1754. https://doi.org/10.1111/j.1365-294X.2005.02527.x.

Peckham, G.W., Peckham, E.G., 1889. Observations on sexual selection in spiders of the family Attidae. Nat. History Soc. Wisconsin 1, 3–60.

Peckham, G.W., Peckham, E.G., 1890. Additional observations of sexual selection in spiders of the family Attidae: with some remarks on Mr. Wallace's theory of sexual ornamentation. Nat. History Soc. Wisconsin 1 (3), 117–151.

Poelstra, J.W., Vijay, N., Bossu, C.M., Lantz, H., Ryll, B., Muller, I., Baglione, V., Unneberg, P., Wikelski, M., Grabherr, M.G., Wolf, J.B.W., 2014. The genomic landscape underlying phenotypic integrity in the face of gene flow in crows. Science 344 (6190), 1410–1414. https://doi.org/10.1126/science.1253226.

Pritchard, J.K., Stephens, M., Donnelly, P., 2000. Inference of population structure using multilocus genotype data. Genetics. 155, 945–959.

Rhymer, J.M., Simberloff, D., 1996. Extinction by hybridization and introgression. Annu. Rev. Ecol. Syst. 27 (1), 83–109. https://doi.org/10.1146/annurev.ecolsys.27.1.83.

Seehausen, O., 2004. Hybridization and adaptive radiation. Trends Ecol. Evol. 19 (4), 198–207. https://doi.org/10.1016/j.tree.2004.01.003.

Shafer, A.B.A., Cullingham, C.I., Côté, S.D., Coltman, D.W., 2010. Of glaciers and refugia: a decade of study sheds new light on the phylogeography of northwestern North America. Mol. Ecol. 19 (21), 4589–4621. https://doi.org/10.1111/j.1365-294X.2010.04828.x.

Shimodaira, H., Hasegawa, M., 1999. Multiple comparisons of log-likelihoods with applications to phylogenetic inference. Mol. Biol. Evol. 16 (8), 1114–1116. https://doi.org/10.1093/oxfordjournals.molbev.a026201.

Smith, B.T., Harvey, M.G., Faircloth, B.C., Glenn, T.C., Brumfield, R.T., 2014. Target capture and massively parallel sequencing of ultraconserved elements for comparative studies at shallow evolutionary time scales. Syst. Biol. 63 (1), 83–95. https://doi.org/10.1093/sysbio/syt061.

Starrett, J., Derkarabetian, S., Hedin, M., Bryson, R.W., McCormack, J.E., Faircloth, B.C., 2017. High phylogenetic utility of an ultraconserved element probe set designed for Arachnida. Mol. Ecol. Resour. 17 (4), 812–823. https://doi.org/10.1111/1755-0998.12621.

Strimmer, K., Rambaut, A., 2001. Inferring confidence sets of possibly misspecified gene trees. Proc. R. Soc. Lond. 269, 137–142.

Stryjewski, K.F., Sorenson, M.D., 2017. Mosaic genome evolution in a recent and rapid avian radiation. Nat. Ecol. Evol. 1 (12), 1912–1922. https://doi.org/10.1038/s41559-017-0364-7.

Taylor, E.B., Boughman, J.W., Groenenboom, M., Sniatynski, M., Schluter, D., Gow, J.L., 2005. Speciation in reverse: morphological and genetic evidence of the collapse of a three-spined stickleback (Gasterosteus aculeatus) species pair: collapse of a stickleback species pair. Mol. Ecol. 15 (2), 343–355. https://doi.org/10.1111/j.1365-294X.2005.02794.x.

Taylor, L.A., Powell, E.C., McGraw, K.J., 2017. Frequent misdirected courtship in a natural community of colorful *Habronattus* jumping spiders. PLoS ONE 12, 1–19.

Toews, D.P.L., Brelsford, A., Grossen, C., Milá, B., Irwin, D.E., 2016. Genomic variation across the Yellow-rumped Warbler species complex. Auk 133 (4), 698–717. https://doi.org/10.1642/AUK-16-61.1.

Turelli, M., Barton, N., 2004. Polygenic variation maintained by balancing selection: pleiotropy, sex-dependent allelic effects and Gx E interactions. Genetics 166 (2), 1053–1079. https://doi.org/10.1534/genetics.166.2.1053.

Wen, D., Yu, Y., Hahn, M.W., Nakhleh, L., 2016. Reticulate evolutionary history and extensive introgression in mosquito species revealed by phylogenetic network analysis. Mol. Ecol. 25 (11), 2361–2372. https://doi.org/10.1111/mec.13544.

Willis, S.C., Farias, I.P., Ortí, G., 2013. Multi-locus species tree for the Amazonian peacock basses (Cichlidae: Cichla): Emergent phylogenetic signal despite limited nuclear variation. Mol. Phylogenet. Evol. 69 (3), 479–490. https://doi.org/10.1016/j.ympev.2013.07.031.

Zhang, J., Cong, Q., Shen, J., Opler, P.A., Grishin, N.V., 2019. Genomics of a complete butterfly continent. bioRxiv. doi: 10.1101/829887.

Zhou, X., Stephens, M., 2012. Genome-wide efficient mixed-model analysis for association studies. Nat. Genet. 44, 821–824.

Zurek, D.B., Cronin, T.W., Taylor, L.A., Byrne, K., Sullivan, M.L.G., Morehouse, N.I., 2015. Spectral filtering enables trichromatic vision in colorful jumping spiders. Curr. Biol. 25 (10), R403–R404. https://doi.org/10.1016/j.cub.2015.03.033.